

Propensity Rules for Angular Momentum Transfer in Electron-Impact Excitation and Deexcitation

K. Bartschat,¹ N. Andersen,² and D. Loveall¹

¹*Department of Physics and Astronomy, Drake University, Des Moines, Iowa 50311*

²*Niels Bohr Institute, Ørsted Laboratory, Universitetsparken 5, DK-2100 Copenhagen, Denmark*

(Received 28 June 1999)

Following the recent investigation of Shurgalin *et al.* [Phys. Rev. Lett. **81**, 4604 (1998)], electron-impact induced $3s \rightarrow 3p$ and $4s \rightarrow 3p$ transitions in atomic sodium are studied theoretically. A propensity rule for the angular momentum transfer is supported for scattering angles below 60° and incident energies below 20 eV. Excellent agreement between the predictions from an R matrix with pseudostates calculation and the experimental data is obtained and provides credibility to the present study.

PACS numbers: 34.80.Dp

Ever since the pioneering discussion by Kohmoto and Fano [1], a parameter of particular interest in the detailed study of atomic collisions has been the so-called “orientation” of the target, which describes the sense of circulation of the active electron(s) around the atomic core. This parameter can be studied in scattered-particle-polarized-photon coincidence experiments, in which the circular polarization P_3 of the light emitted perpendicular to the scattering plane is determined [2]. For the simplest case of $^1S \rightarrow ^1P^o$ excitation without spin exchange and relativistic effects, P_3 , the orientation O_{1-} and the angular momentum transfer L_\perp are related through $P_3 = -2O_{1-} = -L_\perp$. For more complicated situations, the result becomes $P_3 = -fL_\perp$ [2]. The factor f describes depolarization effects due to atomic fine structure and hyperfine structure, cascading if more than one photon can be emitted, and possibly relativistic effects.

Alternatively, the angular momentum transfer can be studied in the “time-reversed” experiment, starting with a laser-prepared state. Following early work by Hertel *et al.* [3,4], this method was further developed by the NIST group [5–7] who generated benchmark data for $3s \rightarrow 3p$ electron-impact excitation in sodium. Subsequently, the technique was widely applied [8–11].

Interestingly, the observed pattern for the angular momentum transfer as a function of the scattering angle showed a characteristic behavior, essentially independent of the collision energy and even the actual target. For electron-impact induced $S \rightarrow P^o$ excitation, almost without exception (see Ref. [12] for a rare example), the value of L_\perp is positive for small scattering angles θ and increases with θ to a maximum beyond which the variation becomes more individual. (See Ref. [13] for an extensive compilation of the available data.) Triggered by these results, considerable effort has been directed into finding a solid theoretical foundation for this empirical propensity rule, the Kohmoto-Fano paper being an early example. Propensity rules for orientation have also been formulated and discussed for heavy-particle impact excitation [14],

and efforts have concentrated on exploring the generality of these rules [15,16].

For electron-atom collisions, a significant step beyond the Kohmoto-Fano work was the analysis by Madison and Winters [17]. After pointing out a phase problem in the Kohmoto-Fano paper, they discussed the orientation parameter in terms of the charge q of the projectile, with $q = \pm 1$ for positron and electron impact, respectively, by expanding the scattering amplitude in a Born series as

$$f_{P \leftarrow S} = \langle \Phi_P | V | \Phi_S \rangle + \langle \Phi_P | VG + V | \Phi_S \rangle + \dots \\ = qt^{(1)} + q^2t^{(2)} + \dots \quad (1)$$

Here V is the interaction potential and G^+ is the free-particle Green’s function with appropriate boundary conditions. This analysis yields

$$L_\perp \propto q^3 \text{Im} \{t_0^{(1)}\} \text{Re} \{t_1^{(2)}\} + q^4 \text{Im} \{t_0^{(2)} t_1^{(2)*}\} + \dots, \quad (2)$$

where the subscript indicates the magnetic quantum number. The first term in this result, involving a product of first-order and second-order amplitudes, dominates at small scattering angles, whereas the second one, a product of two second-order amplitudes, takes over at large angles. Thus, for small scattering angles the orientation parameter should change sign when switching from electron to positron impact, while both projectiles produce orientation parameters of the same sign at larger angles. Madison and Winters confirmed these predictions in a model calculation for the He 2^1P^o state. Concerning the sign of L_\perp at small scattering angles, however, no definitive, general answer could be derived.

A semiclassical argument for the *sign* of the orientation parameter, valid for *small scattering angles*, was outlined by Andersen and Hertel [18]. It is based upon the electrostatic interaction between the projectile penetrating the atomic electron cloud being attractive for electrons but repulsive for positrons. However, this simple argument

neglects the attractive polarization force for electron and positron scattering from neutral targets in their ground state. The analysis of the motion of the active electron around the atomic core suggests that $L_{\perp} > 0$ for electron-impact excitation and $L_{\perp} < 0$ for positrons. Also, changing the sign of the *energy transfer* should reverse the sign of L_{\perp} .

The latter prediction was recently studied in a pioneering experiment by Shurgalin *et al.* [10]. They compared electron-impact excitation of the $3s \rightarrow 3p$ transition in sodium with electron-impact deexcitation of the $4s \rightarrow 3p$ transition. Their results for electron scattering under reversal of the *energy transfer* thus allowed, for the first time, to study the Andersen-Hertel predictions, since the expected signal rates in the corresponding positron experiments are prohibitively small.

Whereas the experiment demonstrated the feasibility of such studies, several open questions remain and justify further study. The experiment was performed for three relatively high incident energies, and the data were restricted to the angular range $4^{\circ} \leq \theta \leq 26^{\circ}$. For the $4s \rightarrow 3p$ deexcitation at an incident energy of 22.0 eV, corresponding to a total (projectile plus target relative to the target ground state) collision energy of 25.2 eV, the experiment indicated that the angular momentum transfer was indeed negative for angles below 18° . For larger angles, however, a significant increase to positive values was observed [10]. The experimental results, as well as those for the “control transition” $3s \rightarrow 3p$, agreed very well with “convergent close-coupling” (CCC) predictions [19], whereas significant deviations were found with those from a “second-order distorted-wave” (DWB2) approach [20]. Similar conclusions were drawn for the higher incident energies of 30 and 50 eV [11]. In light of the satisfactory performance of the DWB2 model for the $3s \rightarrow 3p$ transition, the latter finding might be surprising, since the energy difference of 1.1 eV between the $4s$ and $3p$ states is only about 5% of the incident energy. Hence one might expect a perturbative treatment, especially when carried out to second order, to be sufficiently accurate.

The present Letter reports an extensive study of the Andersen-Hertel predictions by investigating theoretically the above transitions over the full range of scattering angles and a large number of incident energies. While a highly sophisticated numerical method, yielding the expected agreement between theory and experiment, is being used to provide the necessary credibility to this study, we point out that the principal goal is to investigate the validity range of the propensity rule. Nevertheless, as a by-product of our convergence study, we offer an explanation for the difficulties of the DWB2 (and the first-order DWB1 model) in describing the $4s \rightarrow 3p$ transition even at a relatively high incident energy.

We performed several *R*-matrix calculations, ranging in complexity from standard 3-state ($3s, 3p, 4s$), 5-state ($3s, 3p, 4s, 3d, 4p$), and 7-state

($3s, 3p, 4s, 3d, 4p, 4d, 4f$) models to an “*R* matrix with pseudostates” (RMPS) approach. The latter method [21–23] is essentially equivalent to the CCC method, except that it is formulated in an *R*-matrix framework in coordinate space rather than as a close-coupling (CC) method in momentum space. The principal advantage of both CCC and RMPS over standard discrete-state-only treatments lies in the fact that the coupling effect of high-lying discrete states and the target continuum to the states involved in the transition is accounted for by including a large number of square-integrable pseudostates in the close-coupling + correlation expansion of the projectile–target collision system. In our RMPS model, a total of seven *S*-states, seven *P*-states, six *D*-states, and four *F*-states were strongly coupled. Of these states, the lowest seven corresponded to the physical states ($3s, 3p, 4s, 3d, 4p, 4d, 4f$), another four states had energies below the ionization threshold, and the remaining thirteen states represented the target continuum.

Note that the *R*-matrix method is ideally suited for studying a large number of collision energies, due to its efficiency in solving the coupled integrodifferential equations in the interaction regime.

Figure 1 shows L_{\perp} results for electron-impact excitation ($3s \rightarrow 3p$) and deexcitation ($4s \rightarrow 3p$) of sodium as a function of the scattering angle for various collision energies. Whereas reasonable agreement between the experimental data and the theoretical predictions for the excitation process can be achieved already with a simple

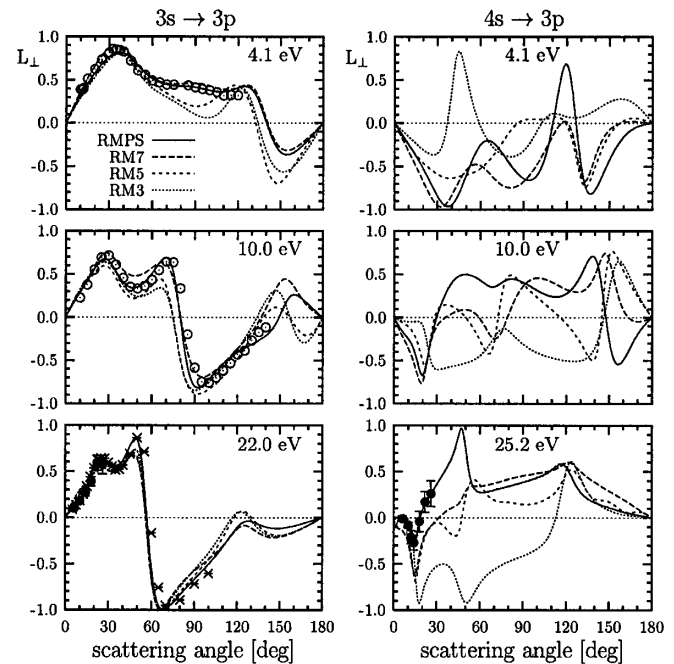


FIG. 1. Angular momentum transfer L_{\perp} for electron-impact excitation and deexcitation of sodium as a function of scattering angle for various collision energies. The predictions from *R*-matrix models (see text) are compared with experimental data from Refs. [6,7] (\circ), [9] (\times), and [10] (\bullet).

three-state CC model (RM3), only the RMPS model is able to reproduce the experimental data for the $4s \rightarrow 3p$ transition. The slow convergence of the CC models for the latter case is consistent with the problems in the perturbative DWB1 and DWB2 models found by Shurgalin *et al.* [10,11].

A possible reason for these problems is illustrated in Fig. 2, which shows the converged RMPS results together with those obtained with a limited number of partial waves. A surprisingly large number of partial waves is required to describe the $4s \rightarrow 3p$ transition at the energies of the Brisbane experiment—just to obtain a definite sign for the result at small angles. (In fact, we cannot rule out the possibility of a numerical artifact being the reason for the dip in our results around 1° .) These partial waves are strongly affected by long-range forces, particularly the polarization of the target by the incident projectile. Whereas approximately 98% of the dipole polarizability of the $3s$ state ($228 a_0^3$ in our calculation) comes from the coupling to the $3p$ state, the theoretical polarizability of the $4s$ state depends strongly on the details of the CC expansion, ranging from $-345 a_0^3$ (RM3) to $+3600 a_0^3$ (RMPS). Although polarization effects are included to leading order in the DWB2 approach, such a strong coupling effect on the dominating partial waves suggests that a perturbative treatment (though converged with the number of partial waves) has not yet converged at the second order of the interaction.

Figure 3 shows L_\perp results for electron-impact excitation ($3s \rightarrow 3p$) and deexcitation ($4s \rightarrow 3p$) of sodium at fixed scattering angles of 10° and 20° as a function of the collision energy. As in Fig. 1, we see the fast ($3s \rightarrow 3p$) and slow ($4s \rightarrow 3p$) convergence of the results with the number of states in the CC expansion. Clearly, the RMPS results support the Andersen-Hertel propensity rule at these small scattering angles and sufficiently low collision energies where the high partial waves are relatively less important than at high energies. The Brisbane result at 20° for 25.2 eV (c.f. Fig. 1) is indeed an exception to the rule because of the high energy.

Figure 4 presents the full set of RMPS results for L_\perp as a function of scattering angle and collision energy for

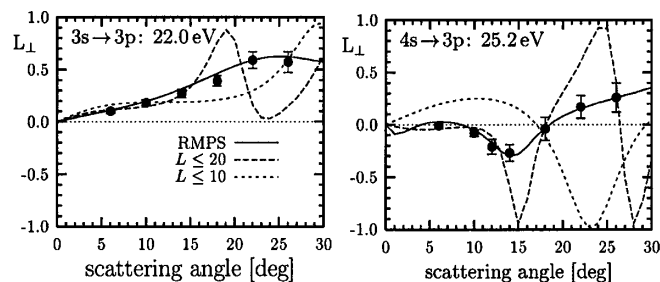


FIG. 2. Partial-wave dependence of the L_\perp results for electron-impact excitation and deexcitation of sodium at small scattering angles. The experimental data are from Ref. [10].

electron impact. Up to angles of about 60° and energies of nearly 20 eV, the propensity rule is quite well fulfilled. For higher energies, however, including those at which the Brisbane experiment was performed [10,11], the validity range of the propensity rule diminishes quickly. The above analysis suggests that the principal reason for this finding is the dominant influence of partial waves with high angular momentum that are strongly affected by the projectile-target distortion.

Finally, we also performed 5-state CC calculations for the two transitions of interest, induced by electron or positron impact. The latter results were obtained with the computer code of McEachran [24]. Because of the possible lack of convergence in the CC expansion and because of the missing positronium formation channel (which, however, is also neglected in the Andersen-Hertel argument), these preliminary results may be regarded as only a qualitative indication. For a collision energy of 6.0 eV, we found that the small-angle propensity rule worked, to a limited extent, for positron-impact deexcitation of the $4s \rightarrow 3p$ transition. This is somewhat expected since, as for the electron-induced $3s \rightarrow 3p$ transition, the projectile charge, the energy transfer, and the attractive long-range interaction all suggest a positive angular momentum transfer at small scattering angles for this case.

In conclusion, we have carried out a comprehensive study of the Andersen-Hertel propensity rule for the angular momentum transfer L_\perp in low-energy electron-impact excitation and deexcitation. Convergent RMPS calculations for the $3s \rightarrow 3p$ and $4s \rightarrow 3p$ transitions in sodium show excellent agreement with the experimental data and support the validity of the propensity rule for low energies in an angular range where (i) partial waves with high angular momenta do not dominate the outcome of the collision, and (ii) the penetration of the target electron cloud by the projectile is insufficient to exhibit the rapidly varying angular dependence of the results. Furthermore, even if

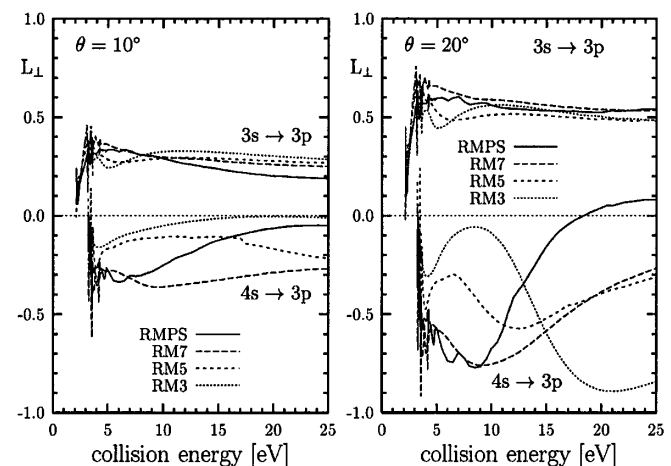


FIG. 3. Angular momentum transfer L_\perp for electron-impact excitation and deexcitation of sodium at scattering angles of 10° and 20° as a function of energy.

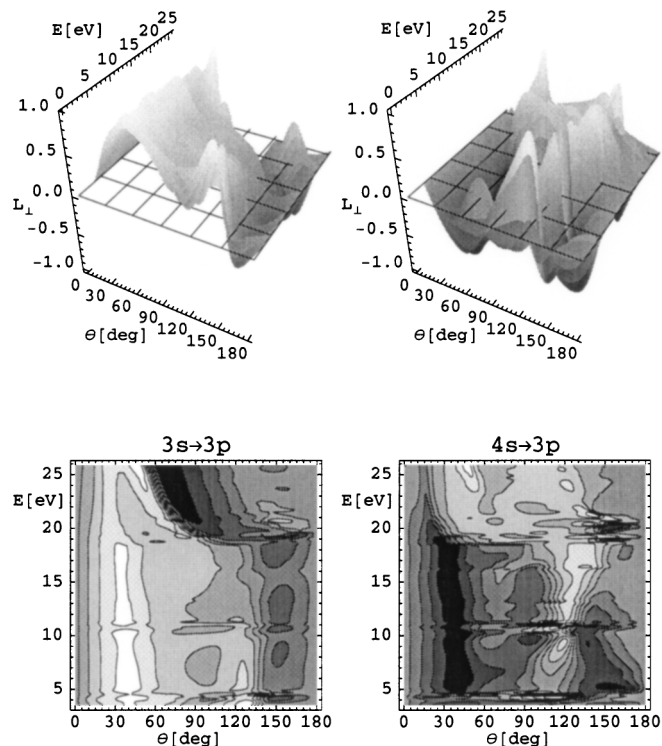


FIG. 4. 3D and contour plots of the RMPS results for L_{\perp} for electron-impact excitation and deexcitation of sodium as a function of scattering angle and collision energy.

high- ℓ partial waves dominate the collision, perturbation-based approximations are likely to face convergence problems in the description of transitions between highly polarizable states. Finally, it is hoped that the present study will stimulate further work on positron-induced transitions for which the positronium formation channel adds additional complexity to the problem.

This work was supported by the United States National Science Foundation (K.B. and D.L.) and the Danish Natural Science Research Council (N.A.).

[1] M. Kohmoto and U. Fano, *J. Phys. B* **14**, L447 (1981).

- [2] N. Andersen, J. W. Gallagher, and I. V. Hertel, *Phys. Rep.* **180**, 1 (1988).
- [3] I. V. Hertel and W. Stoll, *J. Phys. B* **7**, 570 (1974); **7**, 583 (1974).
- [4] J. Macek and I. V. Hertel, *J. Phys. B* **7**, 2173 (1974).
- [5] J.J. McClelland, M.H. Kelley, and R.J. Celotta, *Phys. Rev. Lett.* **55**, 688 (1985); **56**, 1362 (1986).
- [6] J.J. McClelland, M.H. Kelley, and R.J. Celotta, *Phys. Rev. A* **40**, 2321 (1989).
- [7] R.E. Scholten, S.R. Lorentz, J.J. McClelland, M.H. Kelley, and R.J. Celotta, *J. Phys. B* **24**, L653 (1991).
- [8] V. Nickich, T. Hegemann, M. Bartsch, and G.F. Hanne, *Z. Phys. D* **16**, 261 (1990).
- [9] R.E. Scholten, G.F. Shen, and P.J.O. Teubner, *J. Phys. B* **26**, 987 (1993).
- [10] M. Shurgalin, A.J. Murray, W.R. MacGillivray, M.C. Standage, D.H. Madison, K.D. Winkler, and I. Bray, *Phys. Rev. Lett.* **81**, 4604 (1998).
- [11] M. Shurgalin, A.J. Murray, W.R. MacGillivray, M.C. Standage, D.H. Madison, K.D. Winkler, and I. Bray, *J. Phys. B* **32**, 2439 (1999).
- [12] N. Andersen, K. Bartschat, J.T. Broad, G.F. Hanne, and M. Uhrig, *Phys. Rev. Lett.* **76**, 208 (1996).
- [13] N. Andersen, K. Bartschat, J.T. Broad, and I. V. Hertel, *Phys. Rep.* **279**, 251 (1997).
- [14] N. Andersen and S.E. Nielsen, *Europhys. Lett.* **1**, 15 (1986).
- [15] B.W. Moudry, O. Yenen, and D.H. Jaecks, *Phys. Rev. Lett.* **71**, 991 (1993).
- [16] C.D. Lin, R. Shingal, A. Jain, and W. Fritsch, *Phys. Rev. A* **39**, 4455 (1989).
- [17] D.H. Madison and K.H. Winters, *Phys. Rev. Lett.* **47**, 1885 (1981).
- [18] N. Andersen and I. V. Hertel, *Comments At. Mol. Phys.* **19**, 1 (1986).
- [19] I. Bray, *Phys. Rev. A* **49**, 1066 (1994).
- [20] V.E. Bubelev, D.H. Madison, and M.A. Pinkerton, *J. Phys. B* **29**, 1751 (1996).
- [21] K. Bartschat, E.T. Hudson, M.P. Scott, P.G. Burke, and V.M. Burke, *J. Phys. B* **29**, 115 (1996).
- [22] K. Bartschat, E.T. Hudson, M.P. Scott, P.G. Burke, and V.M. Burke, *Phys. Rev. A* **54**, R998 (1996).
- [23] K. Bartschat, *Comput. Phys. Commun.* **114**, 168 (1998).
- [24] R.P. McEachran, in *Computational Atomic Physics*, edited by K. Bartschat (Springer, New York, 1996).